Supporting Information

Toward Supramolecular Nanozymes For The Photocatalytic Activation of Pt(IV) Anticancer Prodrugs

Laura F. Mazzei,[a,b,c] Álvaro Martínez,*[,a] Lucia Trevisan,[c] Daniele Rosa-Gastaldo,[c] Aitziber L. Cortajarena,[b,d] Fabrizio Mancin,*[,c] Luca Salassa*[,a,d,e]

[a] *Donostia International Physics Center, Paseo Manuel de Lardizabal 4, Donostia, 20018, Spain*
[b] *CIC biomaGUNE, Basque Research Technology Alliance, BRTA, Parque Tecnológico de San Sebastián, Paseo Miramón 194, 20014 Donostia/San Sebastián, Spain*
[c] *Dipartimento di Scienze Chimiche, Università di Padova, via Marzolo 1, Padova, 35131, Italy*
[d] *Ikerbasque, Basque Foundation for Science, Bilbao, 48011, Spain*
[e] *Kimika Fakultatea, Euskal Herriko Unibertsitatea, UPV/EHU, Donostia, 20080, Spain*

1. General methods

Materials. Chemicals, solvents and deuterated solvents for NMR were obtained from Sigma-Aldrich and used as purchased without further purification. Ultrapure water was deionised and filtered with a Millipore milliQ system. Thin layer chromatography (TLC) were run on 0.2 mm Macherey-Nagel Alugram Xtra SIL G/UV254 plates and revealed under UV light (λ_{max} = 254 nm) or with phosphomolybdic acid. Column chromatography was performed with silica gel employing Macherey-Nagel Kieselgel 60 with particles sizes of 0.063–0.2 mm (gravity) or 0.04–0.063 mm (flash). Flash columns were performed by applying a positive nitrogen pressure. Glassware in contact with gold nanoparticles was washed with *aqua regia* before and after its use and rinsed with distilled water.

Physical Measurements. DOSY, NOE pumping and NMR spectra for characterization work were acquired on a Bruker 500 MHz Ultra Shield spectrometer, operating at 500 MHz for ^{1}H and 125.7 MHz for ^{13}C. Spectra were calibrated using residual solvent signals according to previously reported values.[1] Catalysis experiments were performed using a Fourier TM Bruker 300 NMR (300 MHz).

ESI mass spectra were recorded on an Agilent Technologies 1100 Series system equipped with a binary pump (G1312A) and MSD SL Trap mass spectrometer (G2445D SL) with ESI source from solutions in methanol or acetonitrile and 0.1% formic acid.

Transmission electron microscopy analysis were run on a FEI Tecnai G12 microscope operating at 100 kV and images registered with an OSIS Veleta 4K camera. TACN AuNPs dissolved in water were deposited on a copper grid and the excess of solvent removed with filtering paper. Size distribution analysis was carried out by modelling nanoparticle intensity profiles employing Gwyddion.[2]

UV-Vis spectra were acquired with a Varian Cary 50 UV-Vis spectrophotometer employing 10 mm path length Hellma Suprasil® quartz cuvettes. Fluorescence spectra were recorded with a Perkin Elmer LS-50B Luminescence Spectrometer. Experiments were conducted at 25°C using a semi-micro fluorescence cuvette with a 10.0x2 mm light path. Samples were excited at 460 nm and the emission at 527 nm was employed for the titration plots.

Thermogravimetric analysis of the thiol-functionalized Au nanoparticles was carried out on *ca*. 1 mg of nanoparticles with a TA Instruments Q5000 IR apparatus. Solvent was removed by heating the sample at 100 °C for 10 minutes and then a 10 °C/min temperature ramp was applied from 100 to 1000 °C.

Nanoparticles were purified by centrifugation on a Hettich Universal 320 R centrifuge operating with a swinging rotor.

Dynamic Light Scattering (DLS) was employed to determine the hydrodynamic diameter of TACN AuNPs. Measurements were performed in a methanol solution containing the nanoparticles (0.3 mg/mL) with 173º scattering angle at 25 ºC using a NanoSizer Malvern Nano-Zs.

2. Synthesis and characterization

Synthesis of 11-(1,4,7-triazonan-1-yl)undecane-1-thiol (TACN-C_{11}-SH)
The TACN-C_{11}-SH ligand was prepared following the procedure described in **Scheme 1**. Previously reported methods were followed for the preparation of compounds **I**,[3] **II**,[4] **III**[5] and TACN-C_{11}-SH.[4]

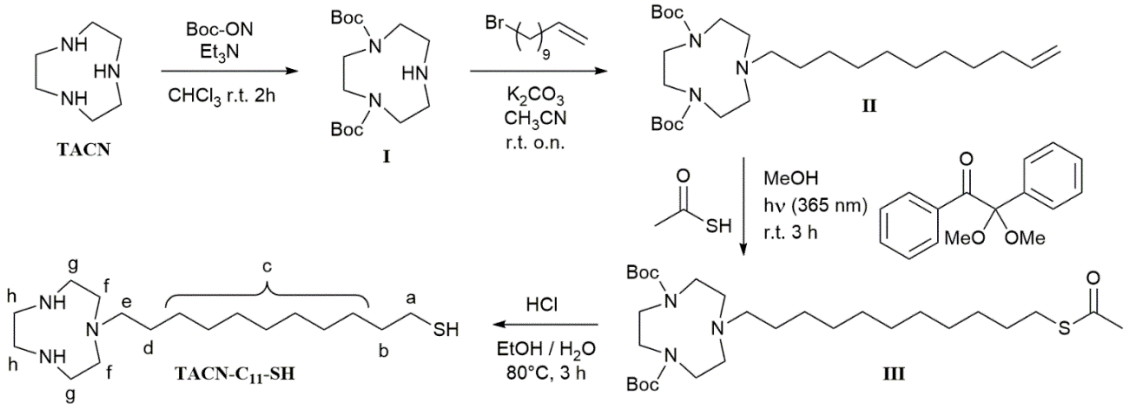

Scheme 1. Synthetic procedure for the preparation of TACN-C_{11}-SH. Letter labels are indicated in the ligand structure for assignment of NMR spectra (Fig. S1).

Di-tert-butyl 1,4,7-triazonane-1,4-dicarboxylate (**I**).
To a solution of 1,4,7-triazacyclononane (TACN) (1 g, 7.74 mmol) in $CHCl_3$ (30 mL) were sequentially added triethylamine (3.2 mL, 23.2 mmol, 3 eq.) and a solution of BOC-ON (3.81 g, 1.58 mol, 2 eq.) in $CHCl_3$ (20 mL) dropwise. The mixture was then stirred at ambient temperature for 2 hours. The solvent was evaporated under reduced pressure, and EtOAc was added to the obtained residue. The organic phase was washed with the following aqueous solutions: 4% $NaHCO_3$, brine and 10% citric acid. The resulting solution was cooled in an ice-bath and NaOH added until pH 10 and became turbid. The mixture was extracted with $CHCl_3$ and the organic portion dried over Na_2SO_4, filtered, and the solvent removed under vacuum to yield a yellow oil. The product was obtained as yellow crystals after freezing overnight at -20 ºC (2.12 g, 83%).

^{1}H NMR (500 MHz, $CDCl_3$), δ (ppm): 3.45 (m, 4H, $H_{(h)}$), 3.29 (m, 4H, $H_{(g)}$), 2.95 (m, 4H, $H_{(f)}$), 1.48 (s, 18H, $C(CH_3)_3$).

Di-tert-butyl 7-(undec-10-en-1-yl)-1,4,7-triazonane-1,4-dicarboxylate (**II**).
To a solution of **I** (400 mg, 1.21 mmol) in 20 mL of CH_3CN, solid K_2CO_3 (201 mg, 1.45 mmol, 1.2 eq.) was added. Afterwards, a solution of 11-bromo-1-undecene (339 mg, 1.45 mmol, 1.2 eq.) in 5 mL of CH_3CN was added and the mixture stirred overnight at 30 °C. The suspension was then filtered and the solvent removed at reduced pressure. The resulting crude oil was purified by flash chromatography in CH_2Cl_2:MeOH 98:2 to yield the desired product (234 mg, 40%).

^{1}H NMR (500 MHz, CD_3OD), δ (ppm): 5.95 – 5.69 (ddt, J = 17.0, 10.2, 6.7 Hz, 1H, -*CH*=CH2), 5.05 – 4.95 (ddt, J = 1.9, 1.6 Hz, 1H, CH=C$H_{(a)}$H$_{(b)}$), 4.91 (ddt, J = 1.2 Hz, 1H, -CH=CH$_{(a)}$*H$_{(b)}$*), 3.46 - 3,50 (m, 4H, $H_{(h)}$), 3.29 – 3.28 (m, 4H, $H_{(g)}$), 2,64 (m, 4H, $H_{(f)}$), 2.59 – 2.42 (m, 2H, $H_{(e)}$), 2.05 (q, J = 6.9 Hz, 2H, -*CH2*-CH=CH2), 1.48 (s, 18H, C(CH3)3), 1.44-1,24 (m, 14H, $H_{(c)}$)

Di-tert-butyl 7-(11-(acetylthio)undecyl)-1,4,7-triazonane-1,4-dicarboxylate (**III**).
Intermediate **II** (100.8 mg, 0.21 mmol), thioacetic acid (57.2 µL, 0.79 mmol, 3.75 eq.) and 2,2-dimethoxy-1,2-diphenylethanone (5.7 mg, 22 µmol, 0.1 eq.) were dissolved in methanol (previously degassed with nitrogen for 20 minutes). The reaction mixture was stirred for 3 hours in a quartz

cuvette under a UV lamp (λ = 365 nm). The crude product was purified by column chromatography in CH_2Cl_2:MeOH 96:4 to give the desired product as a viscous yellow oil (104.75 mg, 95.9%).

^{1}H NMR (500 MHz, $CDCl_3$), δ(ppm): 3.54–3.37 (m, 4H, $H_{(g)}$), 3.32–3.08 (m, 4H, $H_{(f)}$), 2.85 (t, 2H, J = 7.4 Hz, $H_{(b)}$), 2.67–2.53 (m, 4H, $H_{(e)}$), 2.49–2.40 (m, 2H, $H_{(d)}$), 2.32 (s, 3H, CH_3), 1.70–1.06 (m, 36H, $H_{(c)}$, $C(CH_3)_3$).

11-(1,4,7-triazonan-1-yl)undecane-1-thiol **(TACN-C_{11}-SH)**.
To a solution of **III** (104.75 mg, 0.19 mmol) in MeOH (2.5 mL), 6 M aqueous HCl (2.5 mL) was added and refluxed at 80°C for 3 hours. The solvent was removed under reduced pressure to yield the desired thiol as a white solid (68.9 mg, 65.7% yield). The product was used to functionalize the Au nanoparticles immediately after preparation to avoid its oxidation and the formation of disulphides.

^{1}H-NMR (500 MHz, CD_3OD), δ(ppm): 3.55 (s, 4H, $H_{(h)}$), 3.32–3.24 (m, 4H, $H_{(g)}$), 3.08 (t, 4H, J = 5.8 Hz, $H_{(f)}$), 2.88–2.79 (m, 2H, $H_{(e)}$), 2.49 (t, 2H, J = 7.2 Hz, $H_{(a)}$), 1.68–1.53 (m, 4H, $H_{(b)}$, $H_{(d)}$), 1.45–1.24 (m, 14H, $H_{(c)}$). The $H_{(g)}$ signal is covered by the solvent.

$^{13}C\{^1H\}$ NMR (125.7 MHz, CD_3OD), δ (ppm): 57.23 ($C_{(e)}$), 49.47 ($C_{(f)}$), 44.57 ($C_{(g)}$), 43.48 ($C_{(h)}$), 35.22 ($C_{(b)}$), 30.68-28.35 ($C_{(c)}$), 25.56 ($C_{(d)}$), 24.96 ($C_{(a)}$). The $C_{(f)}$ signal is covered by the solvent. ESI-MS, m/z calculated for $C_{17}H_{38}N_3S^+$ $[M+H]^+$ 316, found 315.4.

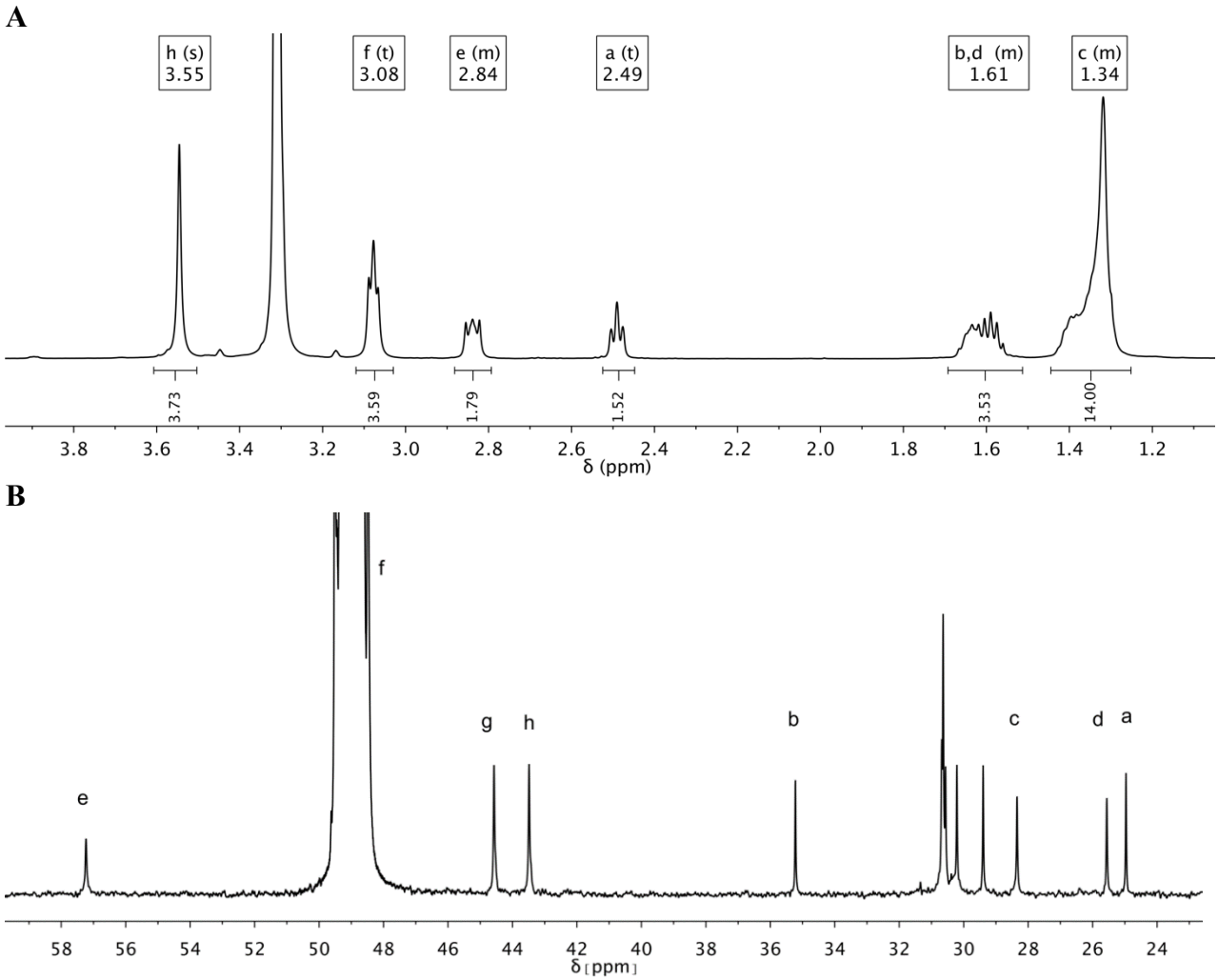

Fig. S1 (A) ^{1}H-NMR and (B) $^{13}C\{^1H\}$ NMR spectra of 11-(1,4,7-triazonan-1-yl)undecane-1-thiol (TACN-C_{11}-SH) in CD_3OD.

Synthesis of Au nanoparticles decorated with TACN-C_{11}-SH ligands (TACN AuNPs).
A modified version of Brust and Schiffrin method was employed for the synthesis of TACN AuNPs.[6] 87 mg of tetraoctylammonium bromide (TOABr) were dissolved in 65 mL of toluene and the solution degassed for 15 minutes with nitrogen. An aqueous solution of $HAuCl_4 \cdot 3H_2O$ (25 mg, 9.9 mM) was extracted with the organic solution and the extract left stirring for 10 minutes under nitrogen. Afterwards, 380 µL of dioctylamine (DOA) were added in one shot and the solution became dark red, brown, green, light yellow and finally colourless. After 2.5 hours, the solution was put in an ice bath and 24 mg of $NaBH_4$ dissolved in 150 µl of milliQ water were added in one shot and the colour of the solution changed to light brown. After 2 hours, the drop of water from the addition of $NaBH_4$ was removed from the reaction mixture with a Pasteur pipette and 21.8 mg of TACN-C_{11}-SH dissolved in 1 mL of methanol were added in one shot. After 10 minutes, the solution became colourless again and TACN AuNPs precipitated. TOABr and DOA were removed through 3 triturations with toluene. Each triturations was carried out by sonicating the NPs suspension for 5–10 min followed by centrifugation at 5000 rpm for 10 min. Afterwards the NPs were purified by size-exclusion chromatography twice (stationary phase: SephadexTM LH-20, eluent: methanol) and the solvent was removed under reduced pressure. The mass of AuNPs obtained was equal to 15.85 mg, yield 68.5% (based on Au).

^{1}H-NMR (500 MHz, CD_3OD), δ (ppm): 3.45–2.70 ($H_{(d)}$, $H_{(e)}$, $H_{(f)}$, $H_{(g)}$), 1.55–1.36 ($H_{(a)}$, $H_{(b)}$, $H_{(c)}$)
TGA: 47.5% (weight loss %)
TEM: 1.9 ± 0.2 nm (average diameter. Number of particles > 250).

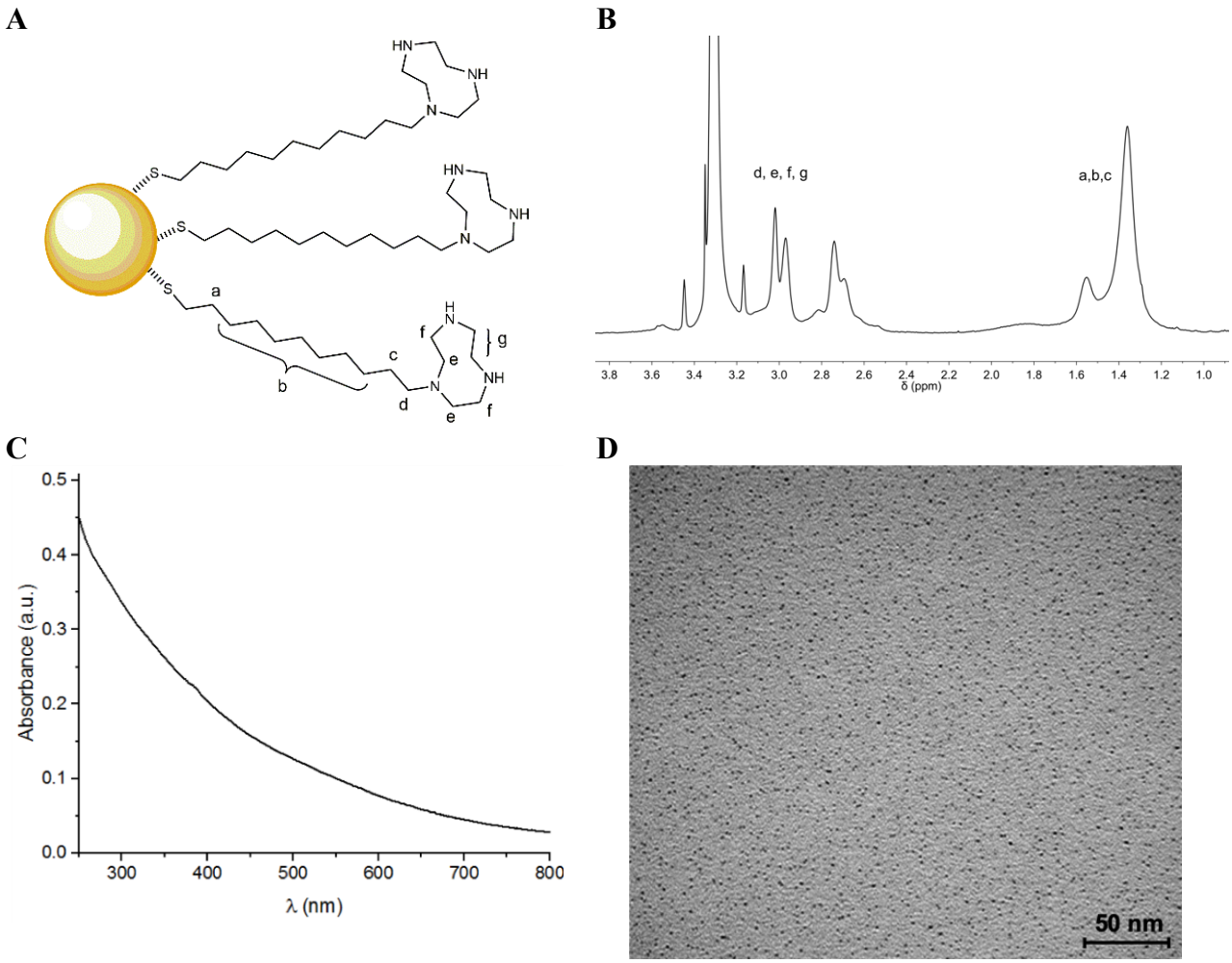

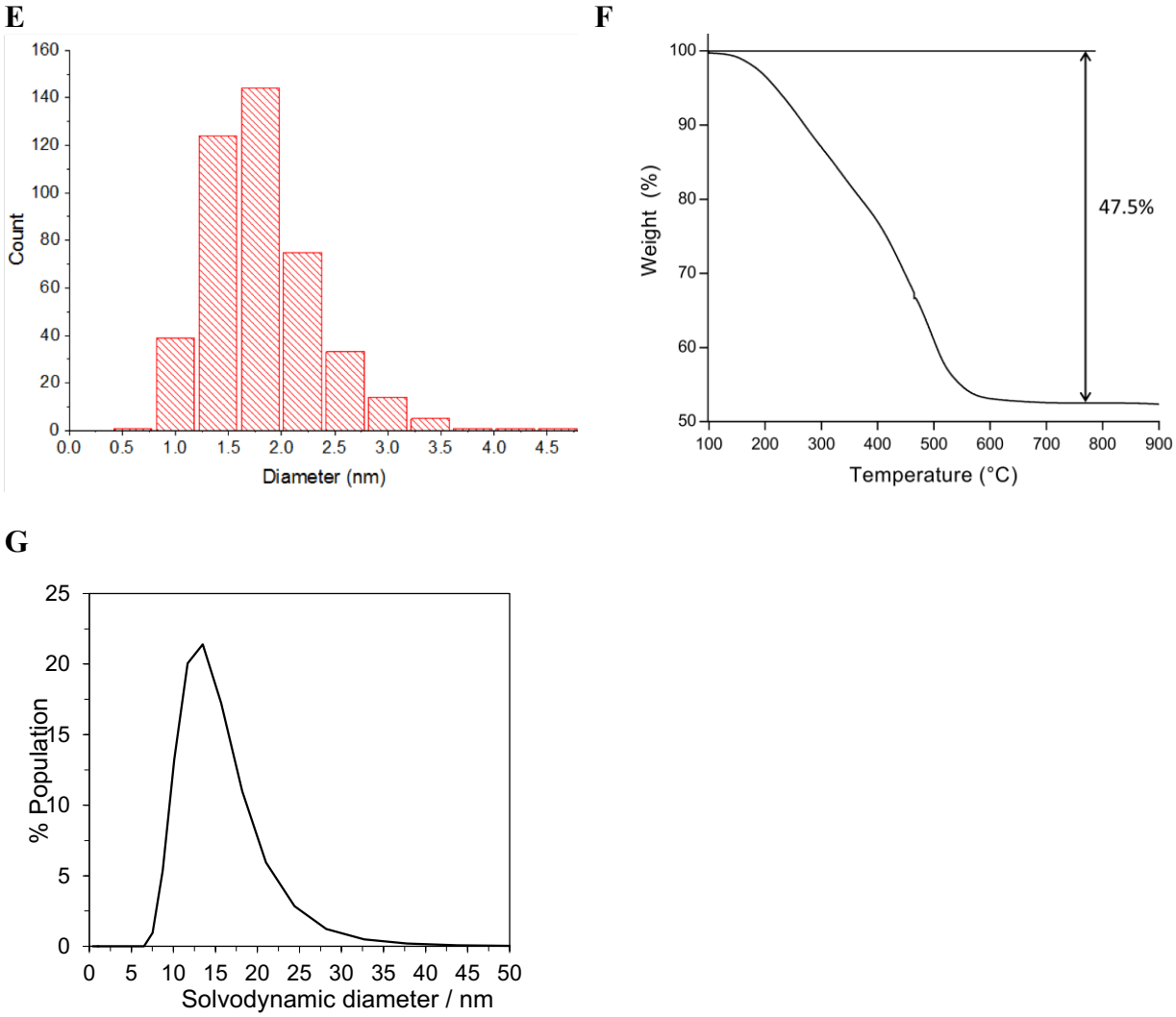

Fig. S2 Characterization of TACN AuNPs: (**A**) Schematic representation with ligand labeling for NMR; (**B**) ^{1}H NMR spectrum in CD_3OD. All the signals present in the spectrum are broad (no free molecules in solution) and correspond to the ones of free TACN-C_{11}-SH by intensity and chemical shift values. The signal corresponding to the methylene group -SCH_2 (2.49 ppm) is not observed in the nanoparticle spectrum due to the large broadening caused by its low mobility; (**C**) UV-Vis spectrum in CH_3OH (0.2 mM); (**D**) TEM micrograph; (**E**) Size distribution histogram (number of particles > 250, average diameter 1.9 ± 0.2 nm); (**F**) TGA thermal curve (47.5 % m/m organic monolayer). From the combined data of TEM and TGA the calculated average formula for the TACN AuNPs used is $Au_{212}SR_{119}$ with a footprint of 0.1 nm^2 per thiol; (**G**) Solvodynamic diameter (14.4 ± 4.0 nm) of TACN AuNPs determined by DLS (number profile).

Determination of thiol concentration in TACN AuNPs.

The thiol mass fraction (w_{TACN}) from the thermogravimetric analysis was employed to assess the concentration of thiols on TACN AuNPs. We calculated the average moles of TACN per mass unit of AuNPs (N_{TACN}/m_{AuNP}) as follows:

$$w_{TACN} = \frac{m_{loss}}{m_{total}} = \frac{m_{TACN}}{m_{AuNP}} \quad \rightarrow \quad \frac{N_{TACN}}{m_{AuNP}} = \frac{\frac{m_{TACN}}{MW_{TACN}}}{\frac{m_{TACN}}{w_{TACN}}} = \frac{w_{TACN}}{MW_{TACN}}$$

DOSY and NOE-pumping experiments.

Diffusion ordered spectroscopy (DOSY) and NOE pumping experiments were carried out in D_2O at 28 ºC. For DOSY spectra [**1**] = 500 µM and $[TACN]_{AuNPs}$ = 2 mM (Figure 2) or [**1**] = 500 µM, $[TACN]_{AuNPs}$ = 100 µM or 1 mM and [FMN] = 25 µM (Figure S4C–E). For NOE pumping conditions were replicated from the literature.[7] In this case [**1**] = 3 mM, $[TACN]_{AuNPs}$ = 1 mM.

3. Loading of FMN – Fluorescence quenching titration measurements

In order to determine the loading of FMN onto TACN AuNPs, we exploited the capacity of Au nanoparticle to quench the emission of a fluorophore in its proximity, due to alteration of the fluorescence intensity created by the electric field of the nanoparticle.[8,9] While incremental addition of FMN without any nanoparticles should result in a linear increase of the emission intensity, when the nanoparticles are present fluorescence intensity should be reduced while FMN is bound to the TACN AuNPs. When concentration of FMN increases beyond the nanoparticle saturation concentration, emission increases due to free FMN in solution. This typically results in two straight lines with a curve region in between the two trends. From the intersection between these two lines an approximate saturation concentration can be retrieved.[10–12]

Correction of the inner filter effect

The inner filter effect is commonly observed in florescence spectroscopy measurements. In highly concentrated solutions, there is a decrease of the fluorophore emission intensity due (i) to strong attenuation of the excitation beam along the optical path, so that only molecules at the surface are excited and fluoresce (primary inner filter), and (ii) to re-absorption of emitted photons (secondary inner filter).[13] Because of the shorter optical path in the emission direction (10x2 mm cuvette) and the little overlap between the absorption and emission spectra of FMN, the secondary filter effect can be neglected in the present case; hence, the corrected fluorescence value (F_{corr}) can be extrapolated determining a correction factor (C) that relates it to the fluorescence intensity observed experimentally (F_{obs}) according to the following semiempirical equations:[13]

$$F_{obs} = F_{corr} \cdot C \qquad C = \frac{\left(e^{-a \cdot d \cdot [FMN]} - e^{-a \cdot [FMN]}\right)}{a \cdot [FMN](1-d)} \qquad F_{corr} = s \cdot [FMN] + F_{blank}$$

$$F_{obs} = (s \cdot [FMN] + F_{blank}) \cdot \frac{\left(e^{-a \cdot d \cdot [FMN]} - e^{-a \cdot [FMN]}\right)}{a \cdot [FMN](1-d)}$$

where [FMN] is the concentration of the fluorophore, F_{blank} is the fluorescence intensity at [FMN] = 0 and a, d and s are parameters to be determined by fitting the experimental fluorescence intensity (F_{obs}) against [FMN].

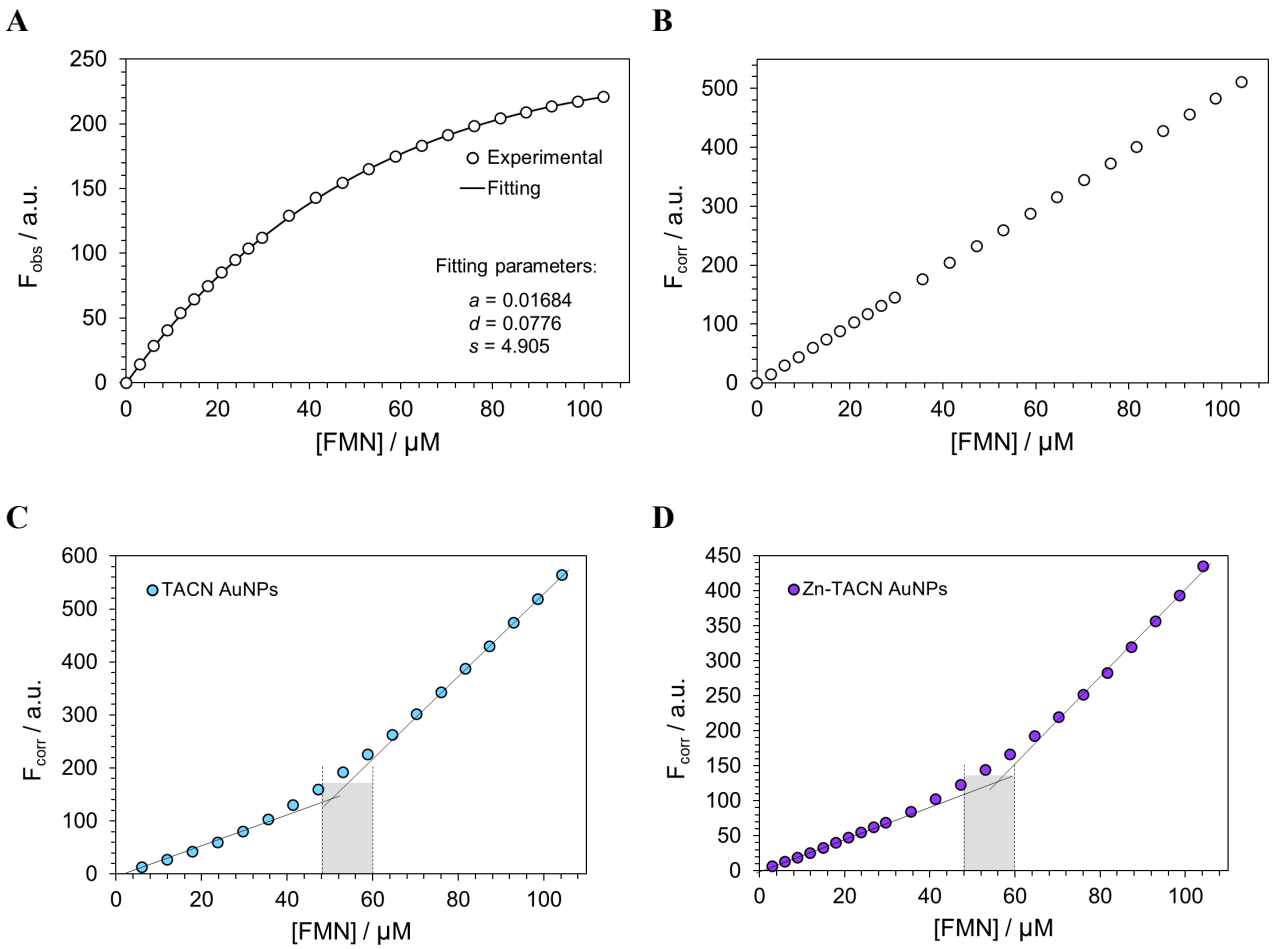

Fig. S3 FMN fluorescence titrations before (**A**) and after inner filter effect corrections (**B**–**D**) for the fluorophore alone and in the presence of TACN AuNPs (100 µM), with or without addition of 1 equivalent of $Zn(NO_3)_2$. The approximate FMN concentration at which the TACN AuNPs binding sites are saturated is obtained at the intersection between the two fitting lines in the graphs **C** and **D** (shadowed rectangle).

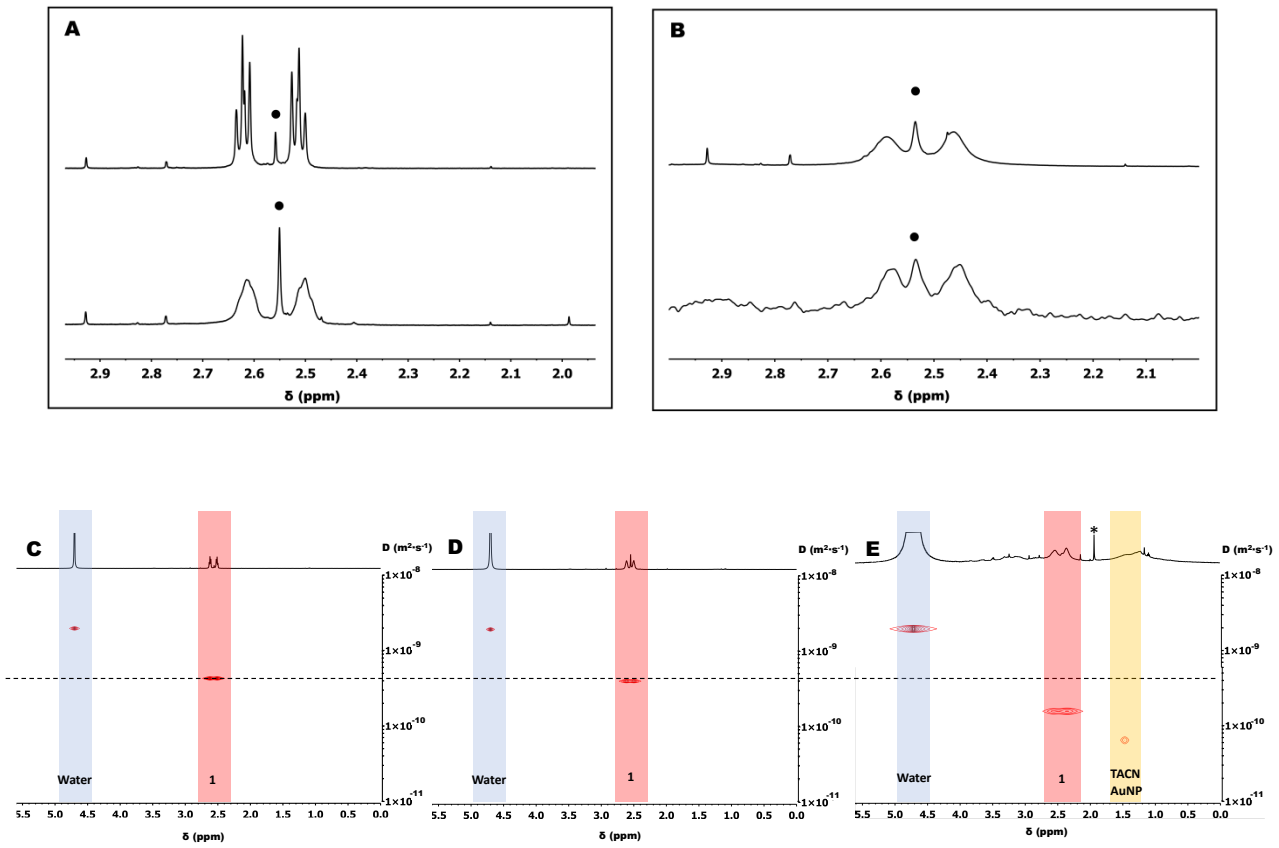

Fig. S4 (**A**) Detail of ^{1}H-NMR spectrum of **1** (500 µM) in absence (upper) and presence (lower) of TACN AuNPs 100 µM and FMN 25 µM. Note how even in presence of a sub-stoichiometric amount of TACN AuNPs the signals of **1** experience a broadening, due to the reduction of the tumbling rate, as expected in the case of **1** binding to the nanoparticles; (**B**) Detail of ^{1}H-NMR spectrum (upper) of **1** (3 mM) in presence of TACN AuNPs (1 mM) and of NOE pumping spectrum (lower) recorded in the same conditions. This magnetization transfer experiment reveals the occurrence of fast exchange interaction between the nanoparticles and the guest. The presence of the signals of **1** in the NOE pumping spectrum confirms the indications obtained from the DOSY and from the ^{1}H-NMR experiments described in **A**. Black circles denote the free succinate signal. (**C–E**) DOSY spectra of **1** (500 µM) in D_2O in absence (**C**) or in presence of 100 µM TACN AuNPs and 25 µM FMN (**D**) or AuNPs 1 mM (**E**). Asterisks denote impurities. In spectrum **D** the signals of TACN AuNPs are not visible. In spectrum **E** only selected signal of the TACN AuNPs is shown for clarity.

Table S1 Diffusion rates of selected signals obtained by the fitting of the decay profiles from the DOSY spectrum of **1** (**Fig. 2A**).

Peak	F2 (ppm)	$I_0 / 10^6$	Error $I_0 / 10^6$	$D / 10^{-10} m^2/s$	Error $D / 10^{-10} m^2/s$
1	4.701	267	0.06	19.4	0.001
2	2.627	1.31	0.04	4.12	0.03
3	2.614	2.68	0.04	4.17	0.02
4	2.601	1.94	0.04	4.15	0.02
5	2.507	1.43	0.04	4.09	0.03
6	2.494	2.19	0.04	4.15	0.02

Table S2 Diffusion rates of selected signals obtained by the fitting of the decay profiles from the DOSY spectrum of **1** in the presence of TACN AuNPs (**Fig. 2B**).

Peak	F2 (ppm)	$I_0 / 10^6$	Error $I_0 / 10^6$	$D / 10^{-10} m^2/s$	Error $D / 10^{-10} m^2/s$
1	4.702	0.321	0.060	19.4	0.0008
2	3.094	0.426	0.037	1.11	0.06
3	2.991	0.374	0.036	0.511	0.06
4	2.721	0.305	0.035	0.372	0.07
5	2.499	0.227	0.036	0.74	0.10
6	2.337	0.496	0.037	1.26	0.05
7	1.232	0.793	0.037	1.20	0.03

Table S3 Diffusion coefficients D ($m^2 \cdot s^{-1}$) of **1** and water from **Fig. S4**.

Spectra	Water (Error $D / 10^{-10} m^2/s$)	1 (Error $D / 10^{-10} m^2/s$)	AuNP (Error $D / 10^{-10} m^2/s$)
C	$1.92 \cdot 10^{-9}$ (0.001)	$4.26 \cdot 10^{-10}$ (0.016)	-
D	$1.92 \cdot 10^{-9}$ (<0.001)	$3.97 \cdot 10^{-10}$ (0.015)	-
E	$1.86 \cdot 10^{-9}$ ((<0.001)	$1.54 \cdot 10^{-10}$ (0.19)	$6.74 \cdot 10^{-11}$ (1.69)

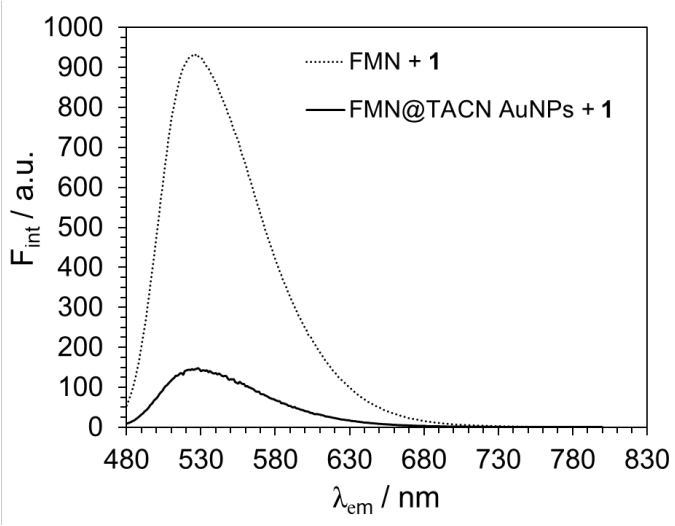

Fig. S5 Fluorescence spectrum of 25 μM FMN in the presence of 500 μM **1** (dotted line) and 100 μM TACN AuNPs plus 500 μM **1** (black line) in MES buffer (5 mM, pH 6).

4. Photocatalysis studies

Photocatalysis experiments

The assays were carried in an NMR tube with a total volume of 600 µL with the following composition: 60 µL (10%) D_2O, 540 µL (90 %) H_2O, 5 mM MES (pH 6.0) 500 µM **1**, 100 µM of TACN AuNPs (with or without 1 equivalent of $Zn(NO_3)_2$), and 25 µM FMN. Samples were irradiated with a custom-made array of blue light emitting diodes (460 nm, 5.30 $mW \cdot cm^{-2}$).[14] Turnover frequency (TOF), turnover number (TON) and % conversion for the catalytic reactions were determined by quantifying the amount of converted Pt(IV) substrate **1** via ^1H NMR. Integration of the free succinato ligand signal (2.25–2.35 ppm) was used for monitoring the reaction progress. TOF values were obtained at substrate conversions of 15–45%.

Catalysis experiments were performed by triplicate and the results reported are the mean of the three measurements ($\overline{x}$). Error bars correspond to the standard errors of each measurement ($\sigma_{\overline{x}}$), calculated as the standard deviation (σ) divided by the square root of the number of measurements (N):

$$\overline{x} = \frac{\sum_{i=1}^{N} x_i}{N} \qquad \sigma = \sqrt{\frac{\sum_{i=1}^{N} (x_i - \overline{x})^2}{N-1}} \qquad \sigma_{\overline{x}} = \frac{\sigma}{\sqrt{N}}$$

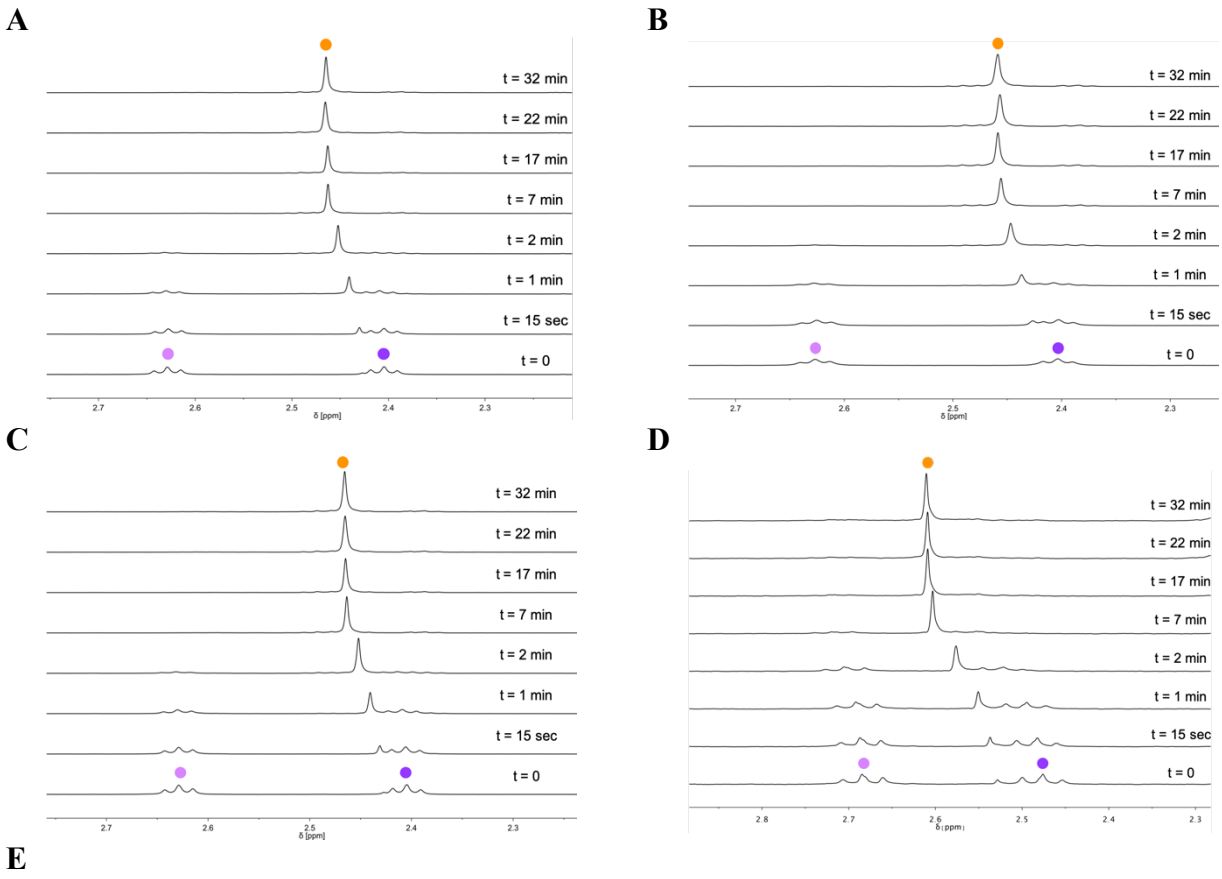

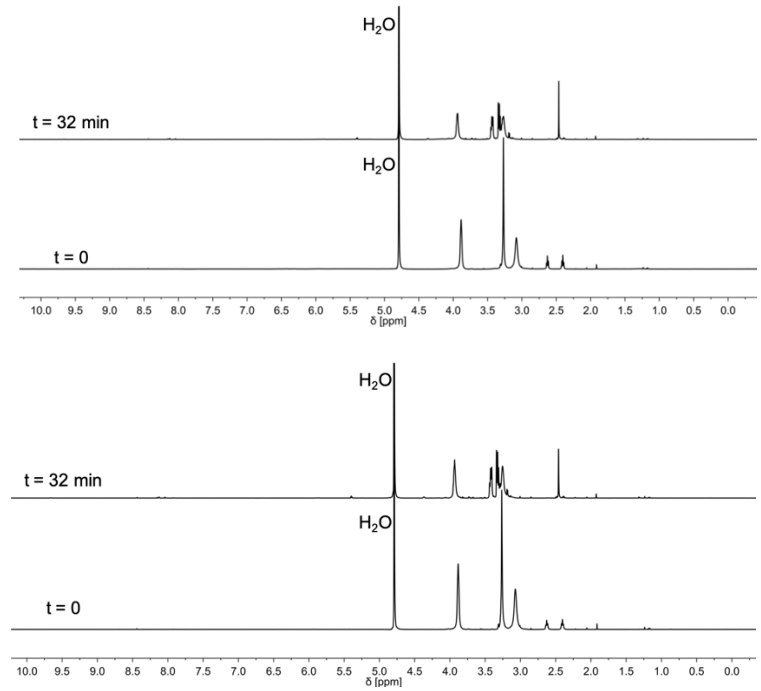

Fig. S6 Photocatalytic activation of **1** by FMN@TACN AuNPs without (**A**) or with (**B**) $Zn(NO_3)_2$, and by free FMN without (**C**) or with (**D**) $Zn(NO_3)_2$ in MES buffer (10% D_2O). **E** and **F** report the full NMR spectra of **A** and **B**. Experimental conditions: [FMN] = 25 μM, [**1**] = 500 μM, $[MES]_{pH\ 6}$ = 5 mM, $[TACN]_{AuNPs}$ = 100 μM, $[Zn(NO_3)_2]$ = 0 μM or 100 μM, hν 460 nm (5.30 mW·cm^{-2}). ^{1}H-NMR signal labelling: ● Pt-OCO**CH$_2$**CH$_2$CO$_2^-$, ● Pt-OCOCH$_2$**CH$_2$**CO$_2^-$, and ● free O$_2$C**CH$_2$CH$_2$**CO$_2^-$.

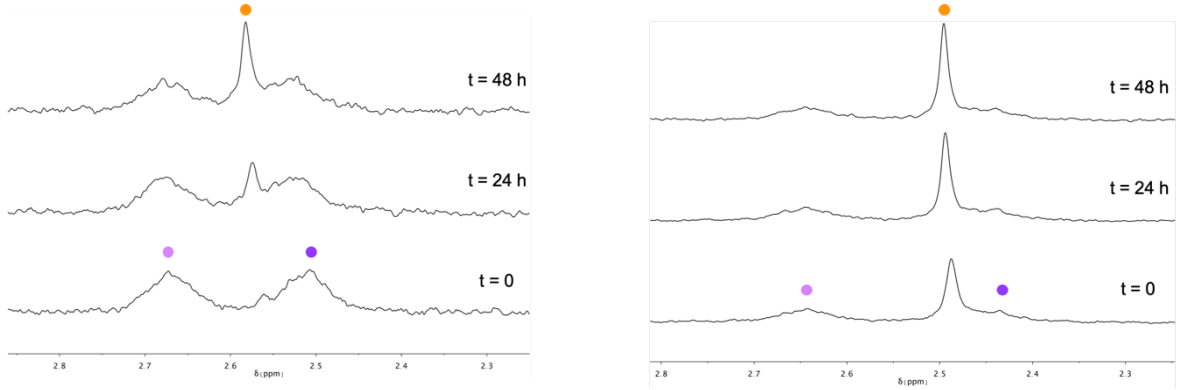

Fig. S7 Dark stability of **1** in the presence of FMN@TACN AuNPs without (**A**) or with (**B**) $Zn(NO_3)_2$, in MES buffer (10% D_2O). Experimental conditions: [FMN] = 25 μM, [**1**] = 500 μM, $[MES]_{pH\ 6}$ = 5 mM, $[TACN]_{AuNPs}$ = 100 μM, $[Zn(NO_3)_2]$ = 0 μM or 100 μM. ^{1}H-NMR signal labelling: ● Pt-OCO**CH$_2$**CH$_2$CO$_2^-$, ● Pt-OCOCH$_2$**CH$_2$**CO$_2^-$, and ● free O$_2$C**CH$_2$CH$_2$**CO$_2^-$.

A **B**

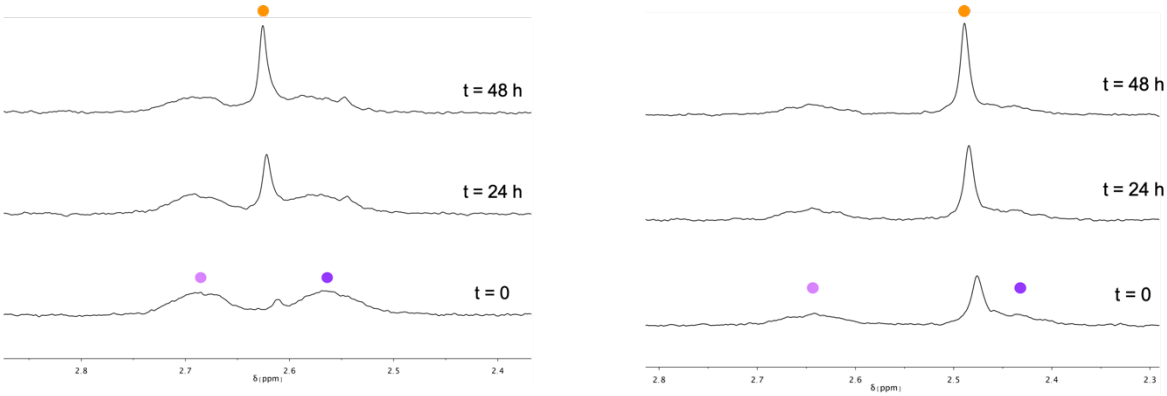

Fig. S8 Dark stability of **1** in the presence of TACN AuNPs without (**A**) or with (**B**) $Zn(NO_3)_2$, in MES buffer (10% D_2O). Experimental conditions: [**1**] = 500 µM, $[MES]_{pH\ 6}$ = 5 mM, $[TACN]_{AuNPs}$ = 100 µM, $[Zn(NO_3)_2]$ = 0 µM or 100 µM. ^{1}H-NMR signal labelling: ● Pt-OCO**CH_2**$CH_2CO_2^-$, ● Pt-$OCOCH_2$**CH_2**CO_2^-, and ● free O_2C**CH_2CH_2**CO_2^-.

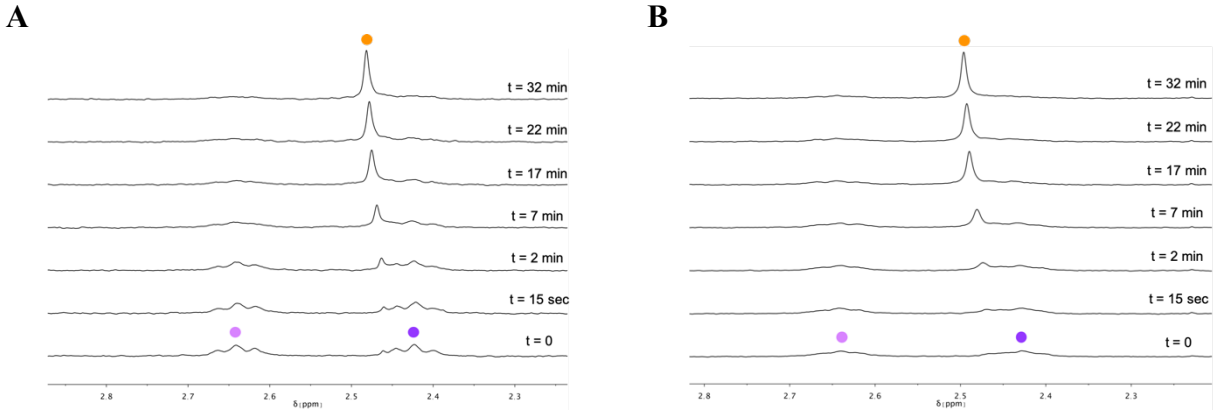

Fig. S9 Photocatalytic activation of **1** by TACN AuNPs without (**A**) or with (**B**) $Zn(NO_3)_2$ in MES buffer (10% D_2O). Experimental conditions: [**1**] = 500 µM, $[MES]_{pH\ 6}$ = 5 mM, $[TACN]_{AuNPs}$ = 100 µM, $[Zn(NO_3)_2]$ = 0 µM or 100 µM, hν 460 nm (5.30 mW·cm^{-2}). ^{1}H-NMR signal labelling: ● Pt-OCO**CH_2**$CH_2CO_2^-$, ● Pt-$OCOCH_2$**CH_2**CO_2^-, and ● free O_2C**CH_2CH_2**CO_2^-.

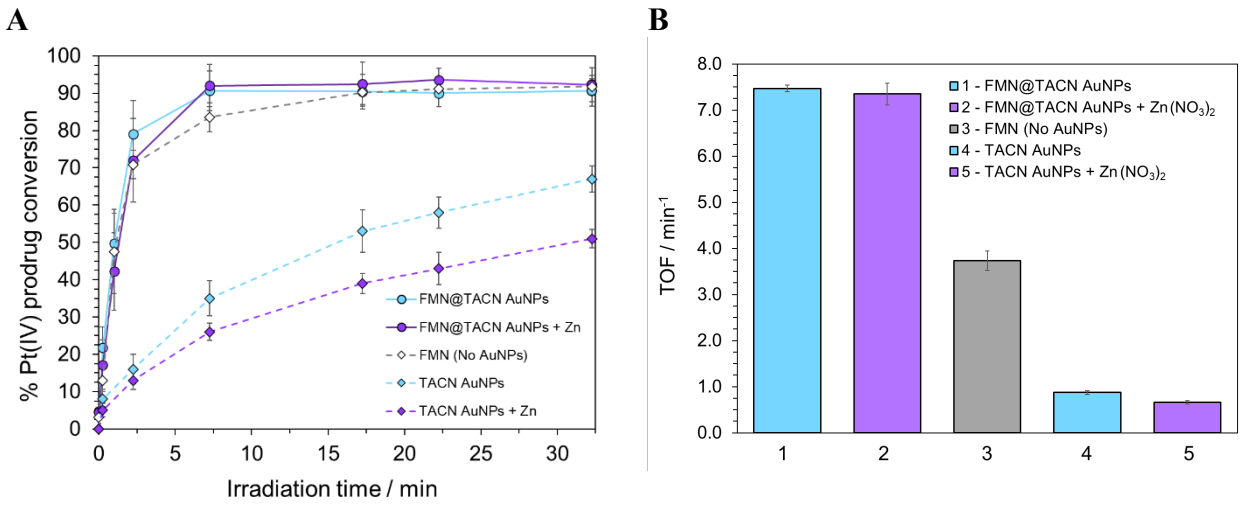

C

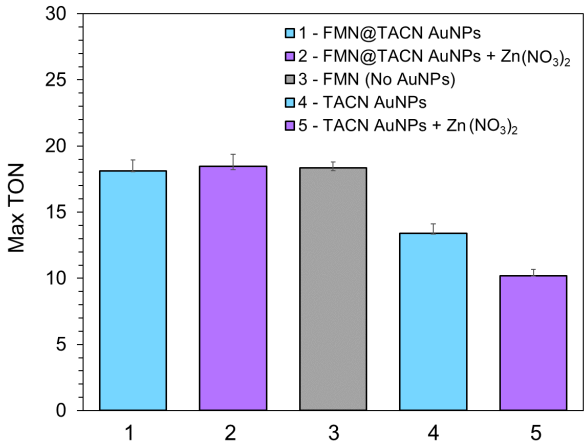

Fig. S10 (**A**) Percentage of activated **1**, (**B**) corresponding TOF values (min^{-1}) and (**C**) TON values reached after 32 minutes of irradiation for FMN, TACN AuNPs, FMN@TACN AuNPs and FMN@Zn-TACN AuNPs in MES buffer. Experimental conditions: [FMN] = 0 or 25 μM, [**1**] = 500 μM, $[MES]_{pH\ 6}$ = 5 mM, $[TACN]_{AuNPs}$ = 0 μM or 100 μM, $[Zn(NO_3)_2]$ = 0 μM or 100 μM, hν 460 nm (5.30 $mW \cdot cm^{-2}$). Each point corresponds to an average of a triplicate measurement.

5. References

1 G. R. Fulmer, A. J. M. Miller, N. H. Sherden, H. E. Gottlieb, A. Nudelman, B. M. Stoltz, J. E. Bercaw and K. I. Goldberg, *Organometallics*, 2010, **29**, 2176–2179.

2 D. Nečas and P. Klapetek, *Cent. Eur. J. Phys.*, 2012, **10**, 181–188.

3 S. Kimura, E. Bill, E. Bothe, T. Weyhermüller and K. Wieghardt, *J. Am. Chem. Soc.*, 2001, **123**, 6025–6039.

4 G. Pieters, A. Cazzolaro, R. Bonomi and L. J. Prins, *Chem. Commun.*, 2012, **48**, 1916–1918.

5 A. K. Tucker-Schwartz, R. A. Farrell and R. L. Garrell, *J. Am. Chem. Soc.*, 2011, **133**, 11026–11029.

6 P. Pengo, S. Polizzi, L. Pasquato and P. Scrimin, *J. Am. Chem. Soc.*, 2005, **127**, 1616–1617.

7 M.-V. Salvia, F. Ramadori, S. Springhetti, M. Diez-Castellnou, B. Perrone, F. Rastrelli and F. Mancin, *J. Am. Chem. Soc.*, 2015, **137**, 886–892.

8 X. Liu, M. Atwater, J. Wang and Q. Huo, *Colloids Surfaces B Biointerfaces*, 2007, **58**, 3–7.

9 S. Chowdhury, Z. Wu, A. Jaquins-Gerstl, S. Liu, A. Dembska, B. A. Armitage, R. Jin and L. A. Peteanu, *J. Phys. Chem. C*, 2011, **115**, 20105–20112.

10 S. Neri, S. Garcia Martin, C. Pezzato and L. J. Prins, *J. Am. Chem. Soc.*, 2017, **139**, 1794–1797.

11 L. Gabrielli, D. Rosa-Gastaldo, M.-V. Salvia, S. Springhetti, F. Rastrelli and F. Mancin, *Chem. Sci.*, 2018, **9**, 4777–4784.

12 F. della Sala, J. L.-Y. Chen, S. Ranallo, D. Badocco, P. Pastore, F. Ricci and L. J. Prins, *Angew. Chemie Int. Ed.*, 2016, **55**, 10737–10740.

13 B. Birdsall, R. W. King, M. R. Wheeler, C. A. Lewis, S. R. Goode, R. B. Dunlap and G. C. K. Roberts, *Anal. Biochem.*, 1983, **132**, 353–361.

14 S. Alonso-de Castro, E. Ruggiero, A. Ruiz-de-Angulo, E. Rezabal, J. C. Mareque-Rivas, X. Lopez, F. López-Gallego and L. Salassa, *Chem. Sci.*, 2017, **8**, 4619–4625.